

## Perspectives on the Physical Chemistry of Semiconductor Nanocrystals

A. P. Alivisatos

Department of Chemistry, University of California, and Materials Sciences Division, Lawrence Berkeley National Laboratory, Berkeley, California 94720

Received: November 30, 1995; In Final Form: March 26, 1996<sup>⊗</sup>

Semiconductor nanocrystals exhibit a wide range of size-dependent properties. Variations in fundamental characteristics ranging from phase transitions to electrical conductivity can be induced by controlling the size of the crystals. The present status and new opportunities for research in this area of materials physical chemistry are reviewed.

The properties of crystalline solids are ordinarily catalogued without reference to their size. It is only in the regime below 10 nm where this variable comes into play. In the past decade, tailoring of materials characteristics by size control has been demonstrated in many inorganic solids belonging to one of the most technologically important classes of materials: semiconductors. For example, in the prototypical material, CdS, the band gap can be tuned between 2.5 and 4 eV, while the radiative rate for the lowest allowed optical excitation ranges from several nanoseconds down to tens of picoseconds.<sup>1</sup> The energy above the band gap required to add an excess charge increases by 0.5 eV,<sup>2</sup> while the very notion of charge transport no longer seems to apply. The melting temperature varies from 1600 down to 400 °C.<sup>3</sup> The pressure required to induce transformation from a four- to a six-coordinate phase increases from 2 to 9 GPa, even as the number of nucleation events for the transition becomes one.<sup>4</sup> This enormous range of fundamental properties is all realized in a material of a single chemical composition: CdS. The variation is achieved by reducing the size of the crystal, not by altering its chemical composition.

There are two major effects which are responsible for these size variations in nanocrystal properties. First, in nanocrystals the number of surface atoms is a large fraction of the total. Second, the intrinsic properties of the interior of nanocrystals are transformed by quantum size effects. In any material, surface atoms make a distinct contribution to the free energy, and the large changes in thermodynamic properties of nanocrystals (melting temperature depression, solid–solid phase transition elevation) can ultimately be traced to this. The surfaces of nanocrystals have until recently been thought of as largely disordered, yielding spherical or ellipsoidal shapes.<sup>5</sup> More recent work shows that nanocrystals assume regular shapes, with the same well-defined facets as are present in extended crystals.<sup>6,7</sup> This opens up the possibility of manipulating the surface energetics of nanocrystals in a controlled manner. The ability to manipulate the energetics of nanocrystal surfaces at will would have practical consequences. To date, nanocrystals are observed to occur in the same crystal structure as the extended solid.<sup>8</sup> It remains an open question whether it will be possible to prepare nanocrystals with interior bonding geometries that do not occur in the known extended solid, by appropriately adjusting the surface energy. Thus, nanocrystals with entirely distinct properties from their extended counterparts may be envisioned.<sup>9</sup> The first part of this review will cover issues related to phase transitions in nanocrystals, with the goal of understanding whether such novel bonding geometries may be stabilized. The second part of the review will cover what is

known about the structure and composition of colloidal semiconductor nanocrystal surfaces.

Independent of the large number of surface atoms, semiconductor nanocrystals with the same interior bonding geometry as a known bulk phase often exhibit strong variations in their optical and electrical properties with size.<sup>10,11</sup> These changes arise through systematic transformations in the density of electronic energy levels as a function of the size of the interior, known as quantum size effects. Nanocrystals lie in between the atomic and molecular limit of discrete density of electronic states and the extended crystalline limit of continuous bands (Figure 1). Now in any material, there will be a size below which there is substantial variation of fundamental electrical and optical properties with size, which will be seen when the energy level spacing exceeds the temperature. For a given temperature, this occurs at a very large size in semiconductors, as compared to metals, insulators, and van der Waals or molecular crystals. This can be understood by considering that the bands of a solid are centered about atomic energy levels, with the width of the band related to the strength of the nearest-neighbor interactions. In the case of van der Waals or molecular crystals, the nearest-neighbor interactions are weak and the bands in the solid are very narrow, and as a consequence not much size variation in optical or electrical properties is expected or observed in the nanocrystal regime. As a function of increasing size, the center of a band develops first and the edges develop last. Thus, in metals, where the Fermi level lies in the center of a band, the relevant energy level spacing is still very small, and at temperatures above a few kelvin, the electrical and optical properties more closely resemble those of a continuum, even in relatively small sizes (tens or hundreds of atoms).<sup>12</sup> In semiconductors, however, the Fermi level lies between two bands, so that the edges of the bands dominate the low-energy optical and electrical behavior. Optical excitations across the gap depend strongly on the size, even for crystallites as large as 10 000 atoms.

The electrical transport properties of nanocrystals also depend strongly on size. The energy required to add successive charges onto an extended crystal does not vary. In a nanocrystal, the presence of one charge acts to prevent the addition of another. Thus, in metals or semiconductors, the current–voltage curves of individual crystallites resemble a staircase, due to this “Coulomb blockade.”<sup>13</sup> Steps in the staircase due to individual charging events are spaced proportional to  $1/\text{radius}$ . These effects have been studied extensively in lithographically prepared semiconductors with lateral dimension of 0.1  $\mu\text{m}$  and in some metal nanocrystals.<sup>14</sup> The electrical characteristics of individual semiconductor nanocrystals, in which Coulomb

<sup>⊗</sup> Abstract published in *Advance ACS Abstracts*, June 15, 1996.

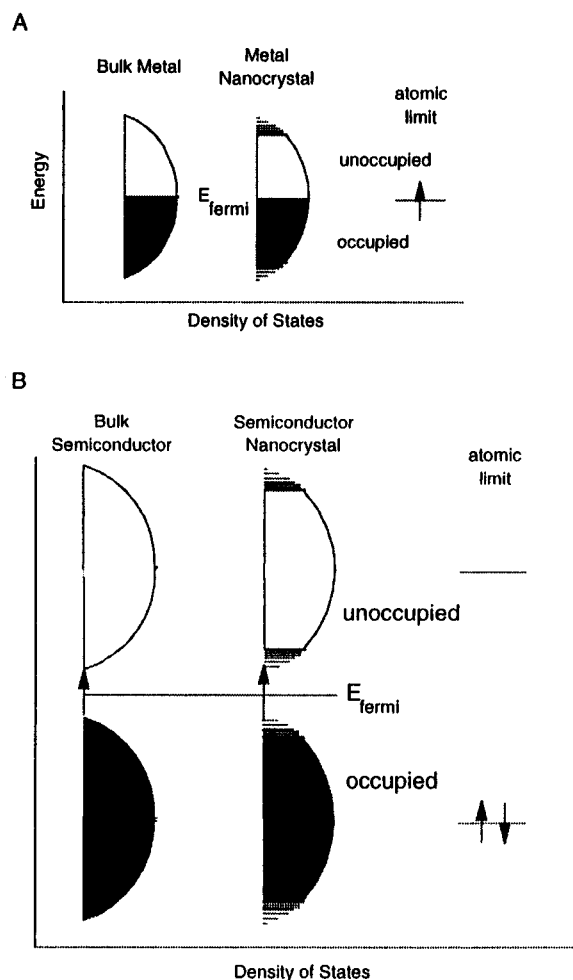


**Figure 1.** Density of states in metal (A) and semiconductor (B) nanocrystals. In each case, the density of states is discrete at the band edges. The Fermi level is in the center of a band in a metal, and so  $kT$  will exceed the level spacing even at low temperatures and small sizes. In contrast, in semiconductors, the Fermi level lies between two bands, so that the relevant level spacing remains large even at large sizes. The HOMO–LUMO gap increases in semiconductor nanocrystals of smaller size.

blockade effects and discrete energy level spacings are both expected to occur, are a topic of much current research.<sup>15</sup> The pronounced variations with size of the optical and electrical properties of semiconductor nanocrystals constitute the final portion of this review.

**Semiconductor Nanocrystal Ideals.**<sup>16</sup> The enormous range of physical properties afforded by size-tuning of semiconductor nanocrystals, in a class of materials with so many established applications in electronics, optics, and sensors, has drawn the attention of scientists from diverse disciplines, from synthetic and physical chemists to materials scientists, condensed matter physicists, and electrical engineers. A direct consequence of the interdisciplinary character of this problem is the diversity of alternative visions for the “ideal” semiconductor nanocrystal. Since none of these ideals have been fully realized, it is of great importance for those working in the field of semiconductor nanocrystals to understand the competing visions, as well as the realities of the samples themselves.

A compositionally pure collection of atoms, mass-selected, isolated in the gas phase, and thermally annealed, is one of the most compelling ideals for a semiconductor nanocrystal.<sup>17</sup> It is in this form that the influence of size alone might be most directly observed. The ability to prepare clusters in the gas phase by laser vaporization must be considered one of the great achievements of cluster science and led to an explosion of work

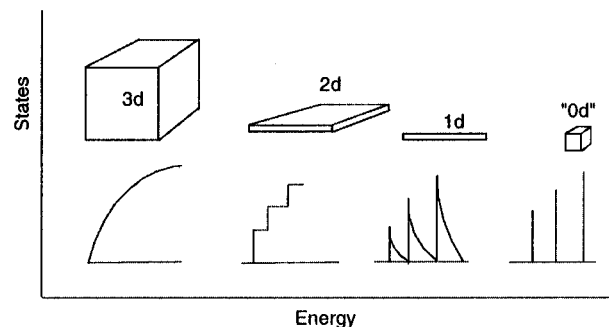


**Figure 2.** Idealized density of states for one band of a semiconductor structure of 3, 2, 1, and “0” dimensions. In the 3d case the energy levels are continuous, while in the “0d” or molecular limit the levels are discrete.

in the field. In the case of semiconductors, early work on bare clusters in the 3–50 atom range has shown that remarkable changes occur in the electronic structure in this regime. As there is no clearly identifiable interior in clusters of this size, it is not too surprising that unique bonding geometries, distinct from those of the bulk solid, are assumed.<sup>18,19</sup> As the size produced and studied in the gas phase continues to increase into the nanocrystal regime, it remains true that this form of cluster is one in which much fundamental science remains to be done. The inability to prepare large quantities of mass-selected nanocrystals by laser vaporization and the difficulties associated with direct measurements of structural properties in the gas phase have also led cluster scientists to pursue other forms of nanocrystals in parallel with the gas phase studies.<sup>20</sup>

Despite the seeming perfection of a pure cluster in the gas phase, from the point of view of semiconductor physics, it is in many ways a highly defective system. At the surface of a pure semiconductor, substantial reconstructions in the atomic positions occur, and there invariably lie energy levels within the energetically forbidden gap of the bulk solid. These surface states act as traps for electrons or holes and degrade the electrical and optical properties of the material. “Passivation” is the chemical process by which these surface atoms are bonded to another material of a much larger band gap, in such a way as to eliminate all the energy levels inside the gap. The ideal termination naturally removes the structural reconstructions, leaving no strain, and simply produces an atomically abrupt jump in the chemical potential for electrons or holes at the interface. The termination of Si with SiO<sub>2</sub> and that of Al<sub>1-x</sub>Ga<sub>x</sub>As with GaAs are probably the best known examples of successful passivation. In the first case the passivation is achieved with a disordered material that can accommodate its local bonding geometry to that of the underlying semiconductor; in the second case the crystal structures and bond lengths of the two materials are matched, so that passivation is achieved epitaxially.

Over decades, the ability to control the surfaces of semiconductors with near atomic precision has led to a further idealization of semiconductor structures: quantum wells, wires, and dots. Ignoring for a moment the detailed atomic level structure of the material, it is possible to imagine simple geometric objects of differing dimensionality (2,1, and 0), in each case made out of homogeneous semiconductor material and with perfect surface termination. Such structures should exhibit the idealized variations in density of electronic states predicted by simple particle in a box type models of elementary quantum mechanics, with the continuous levels of the 3d case evolving into the discrete states of the 0-dimensional case (Figure 2). Phenomenal success has been achieved in making quantum well films of nanometer thick layers of alternating GaAs and Al<sub>1-x</sub>Ga<sub>x</sub>As, using the techniques of molecular beam

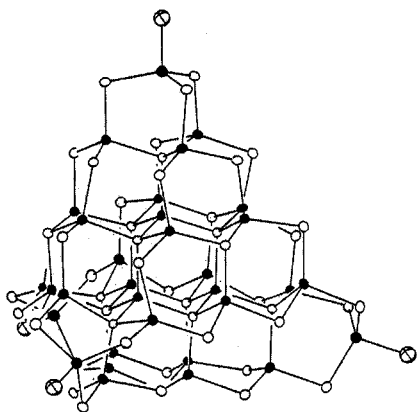


**Figure 3.** Ball and stick model of a  $\text{Cd}_{32}\text{S}_{55}$  molecule recently synthesized and structurally characterized by Herron and Wang.<sup>22</sup> The organic ligands are omitted for clarity. This molecule is a fragment of the CdS zinc blende lattice.

epitaxy. By manipulating steps or defects on a substrate, these same methods can be employed to form wires or, even most recently, dots. One of the most powerful features of these methods is the fact that, at the end, the low-dimensional semiconductor structure is completely embedded inside another material with larger gap, providing a high degree of surface passivation.

A chemist immediately recognizes the zero-dimensional quantum dot as a rather large molecule. Indeed, the third ideal of the nanocrystal derives from a long history of synthetic inorganic cluster chemistry. Chemists have long prepared ever larger inorganic cluster compounds: collections of inorganic atoms bound to each other and surrounded by organic ligands that confer solubility and prevent agglomeration. These clusters are only considered well characterized when they have been crystallized and their structures determined by X-ray diffraction. Unlike any other form of nanocrystal, in this case, the precise atomic composition and the location of each atom are known. In the past decade, chemists have achieved great success in increasing the number of atoms in the inorganic cores of these cluster compounds, to the point where they extend clearly into the nanocrystal regime<sup>21–25</sup> (Figure 3). It is of considerable interest to note that this form of cluster will naturally assume high-symmetry shapes, such as tetrahedral or hexagonal prism.

From the perspective of solid state physics and materials science, it is perhaps surprising that nanocrystals of inorganic solids, coated with organic ligands, may prove one of the most diverse and powerful ideals of a “quantum dot.” This is so because, as a molecule, the nanocrystal can now be considered not just a component embedded in the surface of a solid state device, but rather a *chemical reagent*. In this form the nanocrystal may be dissolved in a fluid, spun into a polymer, attached to an electrical circuit, bound to other nanocrystals as dimers, trimers, etc. or someday perhaps bound to biological molecules. It is important to realize that, in the construction of optical and electronic materials using components of nanometer size, it is not only the physical properties of matter that change but also the chemical methods by which the materials are constructed.

It is not yet established one way or the other whether organic ligands, which turn nanocrystals into chemical reagents, also act as good passivating layers. One difficulty arises in matching the large, bulky ligands required to confer solubility with the compact packing of atoms on the surfaces of the crystallites.<sup>26</sup> Bulky ligands with many torsional modes confer solubility entropically by mixing with the solvent. However, their size ensures that invariably some surface sites are unterminated. *Inorganic* passivation of nanocrystals still is possible, however.

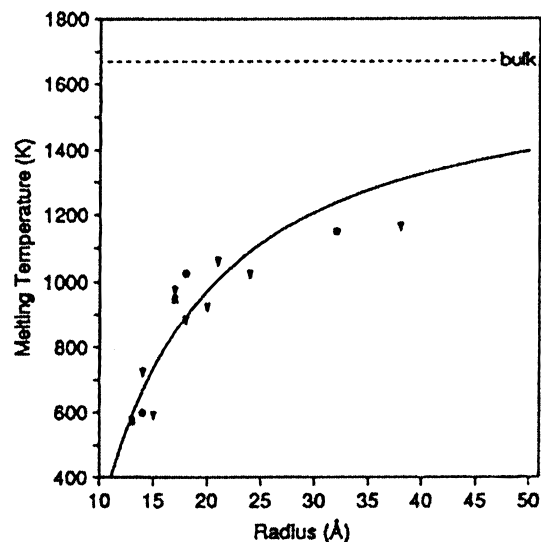


**Figure 4.** Melting temperature versus size for CdS nanocrystals.<sup>3</sup>

This is clearly demonstrated in the case of  $\text{SiO}_2$ -coated Si nanocrystals<sup>27</sup> and in the case of oxidized InP nanocrystals.<sup>28</sup> It is also seen in nanocrystals that are grown inside glass. Indeed, there are even analogs to quantum wells, in which layers of inorganic solids are grown in successive shells around one another, epitaxially. The best documented example of this is the CdS/HgS/CdS quantum dot quantum well.<sup>16,29</sup> In each case, the final product is still small enough that a final layer of ligands bound to the outer surface is sufficient to confer solubility and open the use of these solid state materials to the world of chemical synthesis.

### I. Structural Transformations in Nanocrystals

**The Shape Change Model.** A nanocrystal contains just enough atoms to have an identifiable interior. How does the large number of surface atoms influence the structure of the interior of the nanocrystal? Is it possible in nanocrystals to manipulate the surface so as to trap structures that might ordinarily be unstable in the bulk? To try and place these questions in a well-defined framework, it is important to look at all those transformations in nanocrystals, which, when the radius is extrapolated to infinity, are called phase transitions. In this way one can hope to discover any important scaling laws which relate the bulk phase diagram to the stability of different isomeric structures of nanocrystals.

Previously, only one type of phase transition has been studied extensively in finite systems, both theoretically and experimentally, and that is melting. In a wide variety of materials ranging from metals to semiconductors to insulators, a decrease in solid to liquid transition temperature has been observed with decreasing nanocrystal size.<sup>30–34</sup> A sample of the type of data that can be obtained and the magnitude of the effect are presented in Figure 4 for experiments performed on CdS nanocrystals.<sup>3</sup> Melting point depressions of over 50% are observed for sufficiently small sized nanocrystals. An understanding of this depression can be obtained by considering the factors that contribute to the total energy of a nanocrystal: in a system containing only a few hundred atoms, a large fraction of these atoms will be located on the surface. As surface atoms tend to be coordinatively unsaturated, there is a large energy associated with this surface. The key to understanding this melting point depression is the fact that the surface energy is always lower in the liquid phase compared to the solid phase. In the dynamic fluid phase, surface atoms move to minimize surface area and unfavorable surface interactions. In the solid phase, rigid bonding geometries cause stepped surfaces with high-energy

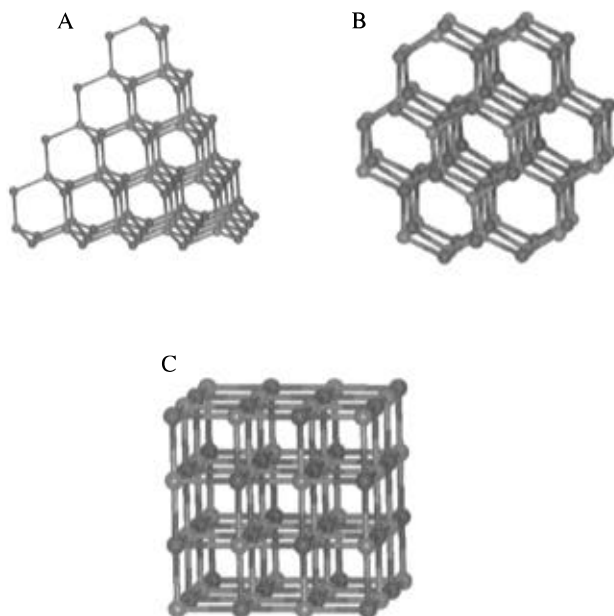


**Figure 5.** Zinc blende (A), wurtzite (B), and rock salt (C) structures. The zinc blende and wurtzite structures are four-coordinate. In the zinc blende structure all the atoms are arranged in "chairs". This structure is favored in covalent semiconductors like InP. Slightly more ionic materials assume the wurtzite structure, in which there are two boats and one chair. The six-coordinate rock salt structure occurs in even more ionic semiconductors like AgBr. Note that in each instance the interior bonding geometry favors a characteristic shape for the entire crystallite: zinc blende, tetrahedral; wurtzite, hexagonal prism; rock salt, cube.

edge and corner atoms. By melting, the total surface energy is thus reduced. This stabilizes the liquid phase over the solid phase. The smaller the nanocrystal, the larger the contribution made by the surface energy to the overall energy of the system and thus the more dramatic the melting temperature depression. As melting is believed to start on the surface of a nanocrystal, this surface stabilization is an intrinsic and immediate part of the melting process.<sup>35,36</sup>

It is of considerable interest to understand whether there are similar scaling laws that apply to solid–solid phase transitions in nanocrystals. Semiconductors such as Si, InP, CdS, and CdSe are all tetrahedrally bonded, with "open" crystal structures (Figure 5). In the more covalently bonded Si or InP, the tetrahedrally bonded atoms can be viewed along any of three axes as sheets of hexagonally shaped chair structures. In the chair arrangement, the repulsion between atoms 180° across the ring is minimized. Thus, the more covalent materials tend naturally to assume tetrahedral shapes characteristic of the diamond and zinc blende interior bonding geometry. In the slightly more ionic CdS and CdSe, the atoms 180° across the rings are of opposite polarity and are attracted Coulombically. Thus, the wurtzite crystal structure with two boats and one chair is more stable. These crystals naturally have hexagonal shapes. Finally, if the ionicity exceeds a critical threshold, as in the silver halides, for example, then the rock salt structure is assumed. When sufficient pressure is applied, all of these materials transform abruptly to more dense crystal structures. The transformation pressure is higher the more covalent the semiconductor: the rather ionic CdS and CdSe transform from the four-coordinate zinc blende or wurtzite structure to the six-coordinate rock salt structure at about 2.5–3 GPa. The less ionic InP transforms again to the rock salt structure at about 10 GPa. Finally, Si in bulk transforms to a series of structures that are slightly distorted away from octahedral symmetry, with the first transformation taking place at about 16 GPa.

In solid–solid transformations, ligands on the nanocrystal

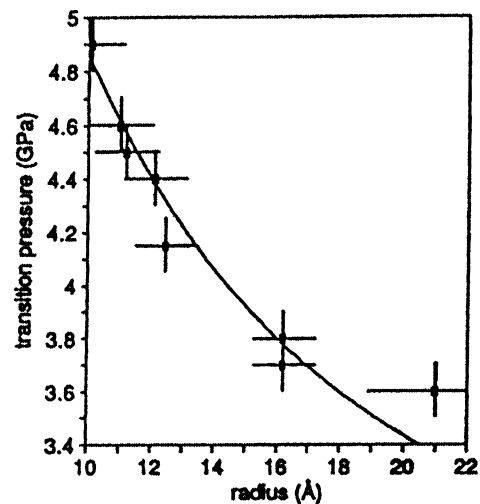


**Figure 6.** Size dependence of the wurtzite to rock salt pressure-induced structural transformation in CdSe nanocrystals.<sup>38</sup>

surface are inevitably present and will influence the observations. They will potentially alter the relative surface energies of the two phases. Studies of solid–solid phase transitions in nanocrystals with differing surface ligands are needed in the future. However, in all nanocrystals studied to date, which include CdS,<sup>37</sup> CdSe,<sup>38</sup> InP,<sup>39</sup> and Si,<sup>40</sup> in all pressure media employed, independent of surface ligand, similar behavior is observed when nanocrystals are subjected to hydrostatic pressure. As the nanocrystals decrease in size, the pressure required to induce transformation to the more dense phase increases (Figure 6, for CdSe), with a scaling law similar to the one that applies to melting, but opposite in direction. Further, in all samples studied to date, the nanocrystals are observed to transform via single nucleation (Figure 7, for CdSe, InP, and Si). This can be seen in the X-ray powder diffraction patterns, which show no broadening upon change of structure. In contrast, bulk single crystals show the effects of multiple nucleation by severe broadening of the X-ray diffraction line widths after the transformation takes place. Furthermore, the structural transformations in nanocrystals are fully reversible, albeit with substantial hysteresis (Figure 8, CdSe). All of these experiments, taken together, suggest that there must be a well-defined pathway by which nanocrystals convert from one structure to another, and understanding this pathway may help uncover the origin of the scaling law.

Let us consider one pathway which takes the nanocrystals from the four-coordinate, tetrahedrally bonded structures to the six-coordinate, octahedrally bonded ones.<sup>41,42</sup> Consider a single sheet of tetrahedrally bonded semiconductor. If the sheet is flattened out, while simultaneously the atoms 180° across from one another are brought closer together, two squares of rock salt will be formed (Figure 9). Further, if this motion is carried out in one ring, then it can be propagated, almost like a zipper closing, all the way across a sheet of the crystal. This normal mode can be viewed in more than one way. The rock salt structure is clearly a higher symmetry structure than the tetrahedrally bonded wurtzite or zinc blende. Indeed, to transform from rock salt to zinc blende or wurtzite requires that the bonds elongate in an alternating way across the sheet. This suggests that these structural transformations may be analogous to Peierls distortions. In polyacetylene it is well-known that the bonds alternate due to a Peierls distortion. Alternating electropositive and electronegative substitutions in polyacetylene will suppress the distortion, because the symmetry is broken electronically and need not be geometrically. Similarly, in three dimensions, NaCl, which is very ionic, is stable in the high-symmetry octahedral rock salt structure. However, C and Si

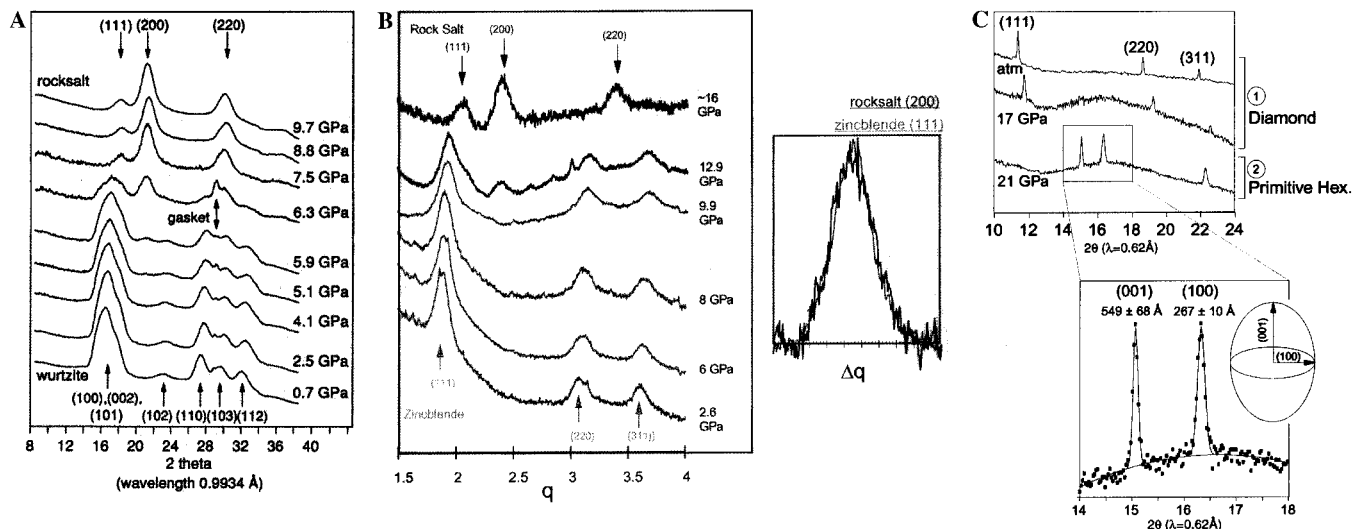


**Figure 7.** (A) Powder X-ray diffraction patterns for CdSe nanocrystals of 44 Å diameter under hydrostatic pressure. The diffraction pattern in the low-pressure, wurtzite, phase is broadened only by the finite size of the crystallites. When the crystallites are dispersed in a soft medium and pressure is applied equally from all sides, they convert from wurtzite (four-coordinate) to rock salt (six-coordinate), with no broadening of the diffraction pattern. (B) High-pressure diffraction data for InP nanocrystals of 50 Å diameter show that these nanocrystals transform from zinc blende to rock salt.<sup>39</sup> The diffraction pattern again shows no broadening (see inset). (C) High-pressure X-ray diffraction data for Si nanocrystals of 50 nm diameter. Again, there is no broadening of the diffraction lines. However, the high-pressure phase diffraction patterns are characteristic of an elongated nanocrystal, providing confirmation of the shape change model.<sup>40</sup>

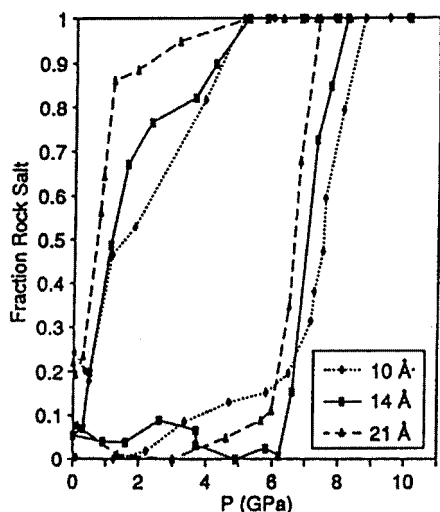


**Figure 8.** Hysteresis in the pressure-induced solid–solid phase transition from wurtzite to rock salt in CdSe nanocrystals.

would be completely unstable in the octahedral form and instead are stable in the diamond structure, which is arrived at from rock salt by bond alternations on two axes. This helps explain why the more ionic semiconductors transform to the octahedral form at lower pressures than covalent ones and why Si at higher pressure avoids the octahedral structure by a series of smaller distortions. Interestingly, Peierls distortion in a one-dimensional polymer leads to no shape change. However, three-dimensional semiconductors must, of necessity, change shape when they undergo this structural transformation. The shape change predicted by this type of Peierls distortion model has in fact been observed for the case of Si nanocrystals.<sup>40</sup> Furthermore, the shape change is the key to understanding the scaling law with size.

Semiconductor nanocrystals, when well formed, are faceted with a defined shape. For example, zinc blende CdS crystallites are tetrahedrally shaped (Figures 14 and 11). Wurtzite CdSe nanocrystals are hexagonal prisms (Figure 10). These shapes reflect the fact that when the crystallites are formed, there is ample opportunity for the atoms to readjust their positions and find the lowest energy ones. However, when the interior

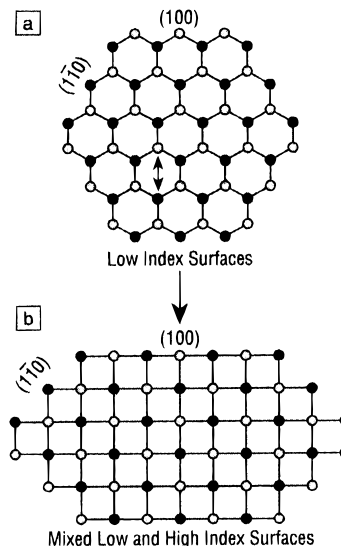
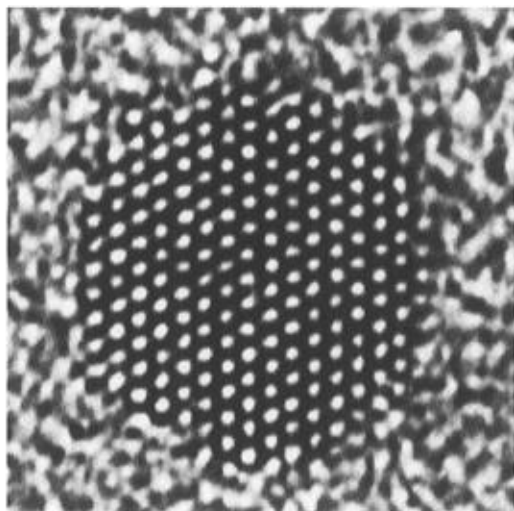


**Figure 9.** Schematic in two dimensions of a possible pathway for the four- to six-coordinate transformations. This pathway naturally takes shape-equilibrated nanocrystals to a high-pressure form with a high-energy shape.

bonding geometry transforms structure from tetrahedral to octahedral, the temperature is low, and there is no possibility for the crystallites to assume their lowest energy shape in the high-pressure phase. For example, in the case of CdSe, this would require a hexagonal prism to transform to a cube, at room temperature. Rather, the final shape is dictated by the pathway of transformation and results in the formation of disordered high-energy surfaces. This explains why the transformation pressure increases in smaller crystallites, where a greater fraction of unstable surface sites must be created. It is a clear illustration of the importance of shape in determining the stability of one structure over another in the nanocrystal regime. In the case of Si (Figure 7c), the high-pressure structure is not as high symmetry, and the shape of the crystallites can be observed directly in the X-ray powder pattern. Finally, these experiments suggest that there may well be pathways of trapping nanocrystals in dense phases that are unstable in bulk (Figure 12). Consider rock salt structure CdSe crystallites. If these are heated at high

A



B

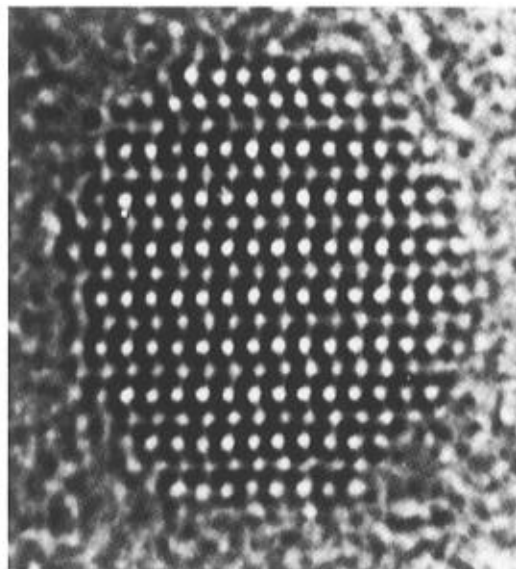


**Figure 10.** (A and B) Transmission electron micrographs of hexagonally shaped wurtzite CdSe nanocrystals.

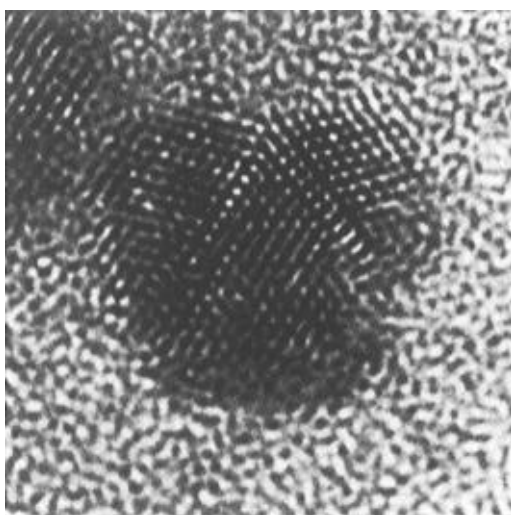


**Figure 11.** Transmission electron micrograph of a tetrahedrally shaped zinc blende CdS nanocrystal upon which subsequent layers of HgS and CdS have been grown epitaxially.<sup>51</sup>

pressure, the shape will anneal to a cube. This cube will then be relatively stable with respect to transformation to the low-pressure tetrahedrally bonded forms, because now the shape change would produce high-index faces of the low-pressure phase. Such experiments to trap high-pressure phases in nanocrystals are underway. In the near future the range of materials accessible in the nanometer size regime will likely exceed what can be prepared in extended solids.

## II. Nanocrystal Surfaces

### Organic Capping: Coverage, Solubility, and Stability.

The surfaces of nanocrystals play a key role in virtually every property, from structural transformations to light emission to solubility. Despite its great importance, the characterization of the composition and the structure of nanocrystal surfaces is in its infancy as compared to the study of plane single-crystal inorganic surfaces. The absence of long-range order requires the development of new techniques, specific to the nanocrystal problem. This is an area of great opportunity, since the large fraction of surface atoms and the observation of well-defined

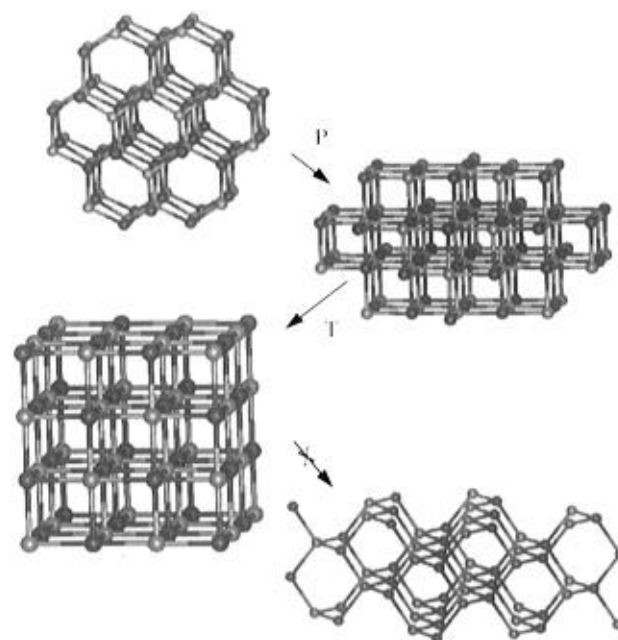


**Figure 12.** A hypothetical sequence of pressurization, heating, cooling, and depressurization, which may lead to metastable nanocrystals trapped in a high-pressure phase.

facets together suggest that it will in fact prove possible to obtain detailed information. Two entirely different types of interfaces need to be considered here: the inorganic/organic interface typically present in a nanocrystal colloid and the solid/solid all inorganic interface of nanocrystals which are embedded completely inside a host material.

Colloidal nanocrystals have a solid/liquid interface, and for the colloid to be soluble and not aggregate, there must be a “cap” molecule at this interface. In the case of semiconductors, CdSe is one of the better characterized systems. Early efforts to study nanocrystal surfaces have included NMR experiments<sup>43–47</sup> as well as X-ray photoelectron spectroscopy (Figure 13A,B).<sup>26,28</sup> These studies present a reasonably consistent picture of the *average* composition of the CdSe nanocrystal surfaces. These colloids are synthesized directly in a hot surfactant, *n*-trioctylphosphine oxide (TOPO).<sup>5,44</sup> At the end

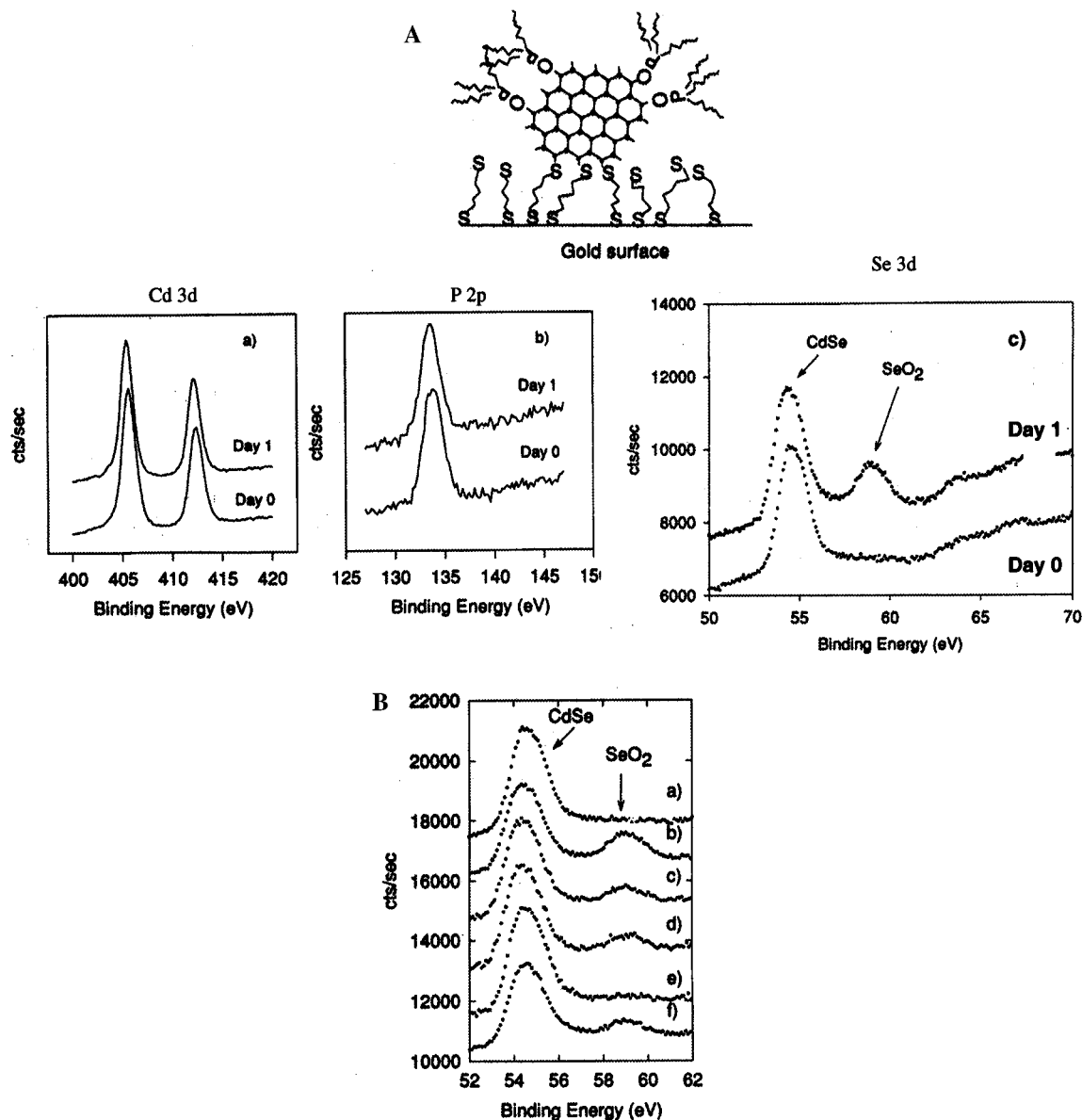


**Figure 13.** (A) X-ray photoelectron spectra of Cd, Se, and P core levels of TOPO coated CdSe nanocrystals. Over a period of 1 day in air, the Se is oxidized.<sup>26</sup> (B) X-ray photoelectron spectra of the Se 3d core level of TOPO-coated CdSe nanocrystals, taken at 1 day intervals. An oxide of Se is formed, which then desorbs, leaving the surface exposed to another cycle of oxidation. This process destroys nanocrystals of II–VI semiconductors which are exposed to both light and oxygen.

of this preparation, the nanocrystals are capped by a monolayer of TOPO, which coordinates to Cd sites. The TOPO molecules are conically shaped and are packed as densely on the nanocrystal surface as the curvature of the surface allows. Thus, the coverage increases with decreasing size, from half of all Cd sites on a flat crystal surface to essentially all Cd sites being capped in a 2 nm diameter crystallite.<sup>26</sup>

The monolayer of TOPO surfactant ensures the solubility of the nanocrystals in nonpolar solvents, like toluene. The phosphine oxide–Cd interaction is relatively weak, and the TOPO can be displaced readily by dissolution in a coordinating solvent, such as pyridine, which interacts even more weakly with the Cd but, because it is a pure solvent, can by mass action displace the TOPO. TOPO-coated nanocrystals of II–VI semiconductors such as CdS and CdSe are unstable with respect to photooxidation. Upon exposure to visible light, the chalcogenide (Se or S) at the surface is oxidized to sulfate or selenate. In turn, this oxide will evaporate from the surface as a molecular species, leaving reduced Cd and a freshly exposed layer of chalcogenide behind<sup>48</sup> (Figure 13B). Nanocrystals of CdSe deposited in a monolayer on a surface and exposed to air and

light are effectively destroyed by these redox cycles within a few days. This has placed definite limits on the use of nanocrystals of II–VI semiconductors in photocatalysis. It is important to note that nanocrystals of III–V semiconductors, such as InP, form stable oxides on the surface, so that their use in electrooptic applications is possible.

The absence of defined shapes in prior samples ensured that studies to date have considered only the *average* coverage of ligands on the nanocrystal. In this situation it is rather difficult to obtain the type of information desired; for example, coverage and structural reconstructions may be very different on some faces than others when the same ligand is present. More studies of faceted crystallites with well-defined shapes may be expected in the future.

**Inorganic Capping of Semiconductor Nanocrystal Surfaces.** There has been widespread interest in the possibility of capping nanocrystals inside an inorganic shell, with organic molecules ligating only the outer surface. In this way, lattice matching can be achieved, and the interface of the nanocrystal can be electronically passivated, while the advantages of solubility and chemical manipulation are maintained.<sup>49</sup> Interest

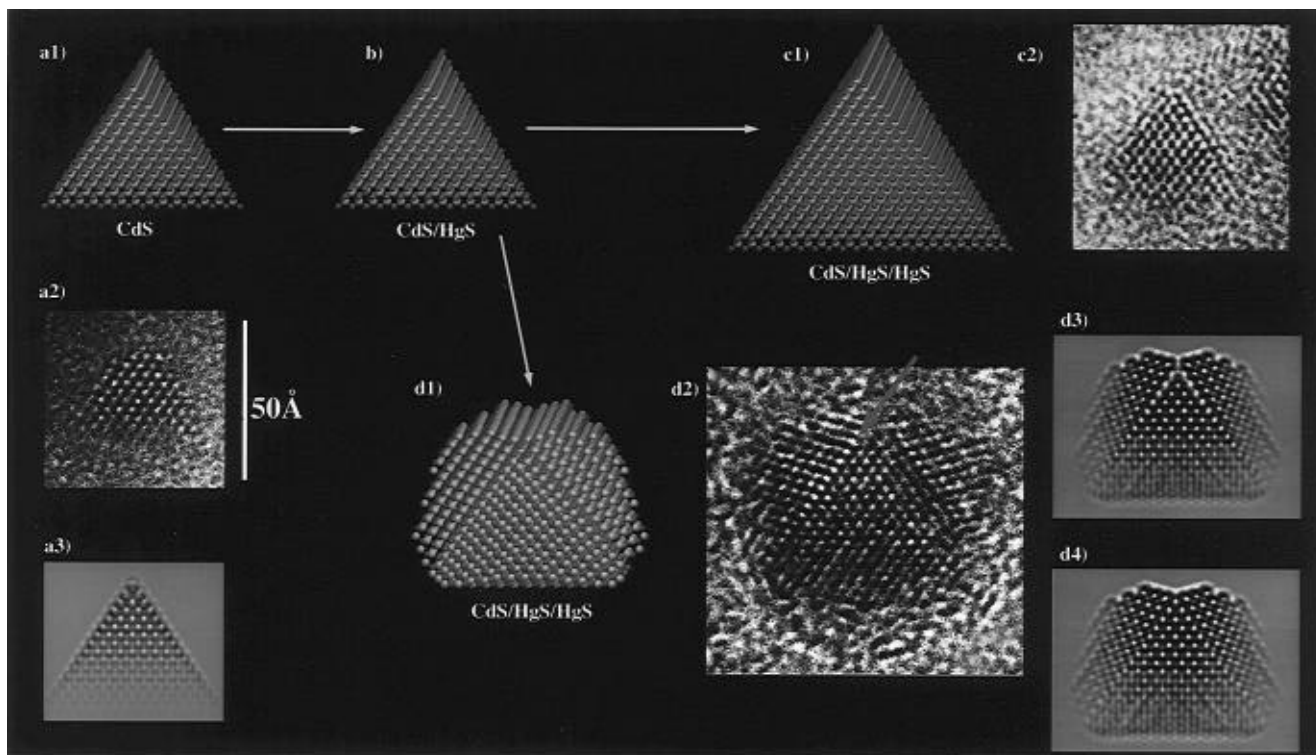


**Figure 14.** Transmission electron microscopy study of the growth of a CdS/HgS/CdS quantum dot quantum well.<sup>51</sup> The micrograph of a CdS core cluster (a2) exhibits tetrahedral morphology which is in agreement with TEM simulation (a3). The corresponding molecular model (a1) shows that all surfaces are Cd terminated (111). Picture b shows a model of the CdS particle after surface modification with Hg. A typical micrograph of a tetrahedral CdS/HgS/CdS nanocrystals is shown in (c2) along with a corresponding model (c1). Model (d1) and micrograph (d2) represent a CdS/HgS/CdS nanocrystal after twinned epitaxial growth. The arrow marks the interfacial layer exhibiting increases contrast due to the presence of HgS, in agreement with the simulation (d3). No contrast is seen in a simulation of a model with all Hg replaced by Cd (d4).

in this concept is increasing for two reasons: the recent observation that luminescence yields are greatly enhanced in ZnS-capped CdSe nanocrystals<sup>50</sup> and the development of faceted nanocrystal samples.<sup>51,67</sup> In faceted crystallites, it is possible to imagine performing precise epitaxial growth on specific crystallographic faces of a particle, something that would be a great deal more difficult in a rounded, but surface disordered, crystallite.

An example of inorganic capping is afforded by the CdS/HgS/CdS quantum dot quantum well of Weller and co-workers. A nanometer size shell of HgS is completely embedded inside CdS layers. The sequence by which this nanocrystal heterostructure is constructed is illustrated in Figure 14. CdS nanocrystals are synthesized in water at room temperature. Under these conditions, the nanocrystals are zinc blende interior bonding geometry and tetrahedrally shaped. These nanocrystals are faceted, with only one crystallographic face exposed, which is almost ideal for epitaxy. Upon exposure of the nanocrystals to Hg<sup>2+</sup> ions, the outermost layer of Cd is displaced from the surface, because HgS has a lower solubility than CdS. Subsequently, more CdS is grown on top of this HgS layer. Either the final structure is still completely tetrahedral (Figure 14, c2) (in which case all the surfaces are epitaxially grown), or else the more complex morphology of Figure 14, d2 is observed. In this latter case, a stacking fault has occurred at the HgS/CdS interface, and the complete tetrahedron cannot form because the adjacent faces are growing out of phase. The ability to control faceting and epitaxy in colloidal nanocrystal heterostructures will remain an extremely active area of research in the near future.

### III. Quantum Size Effects

The most striking property of semiconductor nanocrystals is the massive changes in optical properties as a function of the

size.<sup>10,11</sup> As size is reduced, the electronic excitations shift to higher energy, and there is concentration of oscillator strength into just a few transitions. These basic physical phenomena of quantum confinement arise by changes in the density of electronic states and can be understood by considering the relationship between position and momentum in free and confined particles:

$$\Delta p \Delta x \geq \hbar/2$$

For a free particle or a particle in a periodic potential, the energy and the crystal momentum  $\hbar k$  may both be precisely defined, while the position is not. As a particle is localized, the energy may still be well-defined; however, the uncertainty in position decreases, so that momentum is no longer well-defined. The energy eigenfunctions of the particle may then be viewed as superpositions of bulk  $k$  states. In the extended case, there is a relationship between energy and momentum, and to a first approximation, the change in energy as a function of the size can be estimated simply by realizing that the energy of the confined particle arises by superposition of bulk  $k$  states of differing energy.

For a free particle, the dependence of energy on wavevector is quadratic:

$$E = \hbar^2 k^2 / 2m$$

In the effective mass approximation, this relationship is assumed to hold for an electron or hole in the periodic potential of the semiconductor, with a reduced mass which is inversely proportional to the width of the band. Given the relationship between confinement in space and momentum superposition, this leads directly to the approximate dependence of energy on size as  $1/r^2$ , as expected for a simple particle in a box. For large sizes, the approximation is nearly correct but breaks down



for even moderately sized because energy does not depend quadratically on  $k$  in real crystallites.

To gain a physical understanding of the variation of  $E$  with  $k$ , it is at this point useful to switch to a molecular picture of bonding in the solid (15A) and of the quantum confinement process. The single-particle wave functions for electrons and holes in the extended solid can be viewed as linear combination of unit cell atomic orbitals, multiplied by phase factors between the unit cells. When all the cells are in phase, the wavevector,  $k = (2\pi/\lambda)$ , is equal to 0; when adjacent cells are out of phase,  $k$  takes on its maximum value,  $\pi/a$ . In a simple one-dimensional single band tight binding model, the dependence of  $E$  on  $k$  is

$$E = \alpha + 2\beta \cos(ka)$$

where  $\alpha$ , the energy of the linear combination of atomic orbitals inside the unit cell, determines the center position of the band in energy.  $2\beta$  gives the width of the band and is directly related to the strength of nearest-neighbor coupling and inversely proportional to the effective mass. An expansion of the  $\cos(ka)$  term for small  $k$  yields a quadratic term as its first term, so that one can see why the effective mass approximation only describes the band well near either its minimum or its maximum.

Considering now a real binary semiconductor, such as CdSe, the single particle states can be viewed as products of unit cell atomic orbital combinations and phase factors between unit cells (Figure 15A). For example, the highest occupied molecular orbital or top of the valence band may be viewed as arising from Se 4p orbitals, arranged to be in phase between unit cells. This will be the maximum of the valence band, since adjacent p orbitals in phase are  $\sigma$  antibonding (and  $\pi$  bonding). Similarly, the lowest unoccupied molecular orbital will be comprised of Cd 5s atomic orbitals, also in phase between unit cells. This is the minimum of the conduction band, since s orbitals in phase constructively interfere to yield a bonding level. In this case, the minimum of the conduction band and the maximum of the valence band have the same phase between unit cells.

How does optical absorption arise in the extended solid? The optical absorption matrix element is given by

$$\mu = \langle \text{Cd } 5s | e r | \text{Se } 4p \rangle \langle \psi_{i,\text{vib}} | \psi_{i,\text{vib}} \rangle \langle \exp(ik_c r) | \exp(ik_v r) \rangle$$

where  $\exp(ikr)$ , the envelope functions, denote the phase factors between unit cells, and the vibrational overlap between ground and excited vibrational states is determined by Franck–Condon factors, just as for allowed transitions in molecules. Note that in this case the electronic transition between the unit cell functions is dipole allowed. The radiative rate is determined from

$$w = \int_f \frac{2\pi}{\hbar} |\mu|^2 \delta(E_f - E_i + E_{\text{photon}}) \rho(E_f, E_i) dE$$

where  $\rho$  denotes the joint density of valence and conduction band electronic states with the same  $k$ . The matrix element is factored so that the dipole operator acts on the electronic wave function within the unit cell, and the phase factors between unit cells,  $\exp(ik_v r)$  and  $\exp(ik_c r)$ , must overlap for the transition to be allowed ( $k_v = k_c$ ). In this case, the transition is dipole allowed within each unit cell. Further, the transition dipole moment points in the same direction from unit cell to unit cell. Thus, the electric field of light, which is very long wavelength compared to the size of the unit cell, can drive all the transition dipoles in phase, and overall the transition is allowed. In the language of solid state physics, this is a vertical transition, with  $\Delta k = 0$ , and hence CdSe is called a direct band gap material. At low temperature, the electronic transition will be accompanied by vibrational excitation of totally symmetric modes,

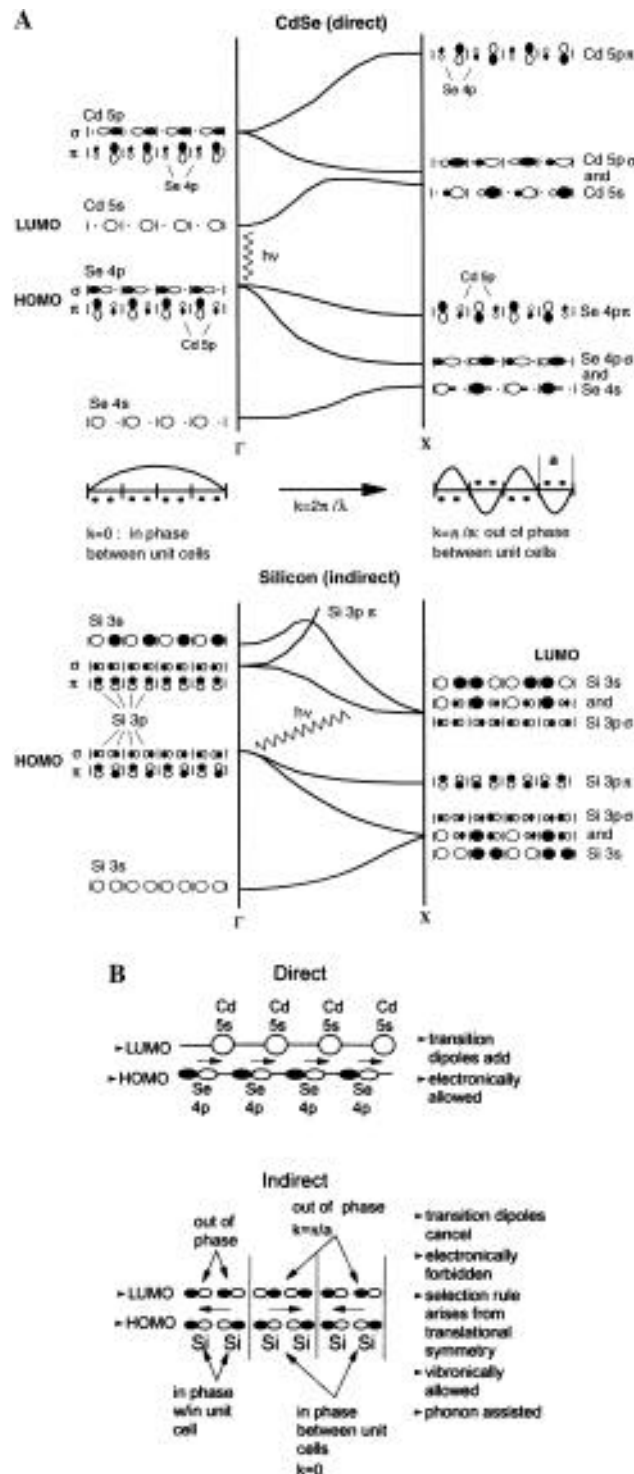


**Figure 15.** (A) A simplified MO diagram for the electronic structures of zinc blende CdSe and diamond structure Si. (B) A comparison of the HOMO–LUMO transitions for CdSe and Si. In CdSe the transition is dipole allowed, while in Si it is not.

in accordance with the Franck–Condon factors. Past the absorption threshold, the unit cell matrix element for absorption is largely unchanged, and the absorption efficiency rises steeply at higher incident photon energies because of the large increase in the joint density of states for vertical transitions. Numerous experiments show that quantum confinement dominantly affects the absorption spectrum by changes in the envelope functions and the density of states as a function of the energy, with relatively less effect on the intrinsic, unit cell based, matrix element for absorption.

**Quantization and Energy Level Spacing.** Now one may consider nanocrystals of direct gap semiconductors, such as

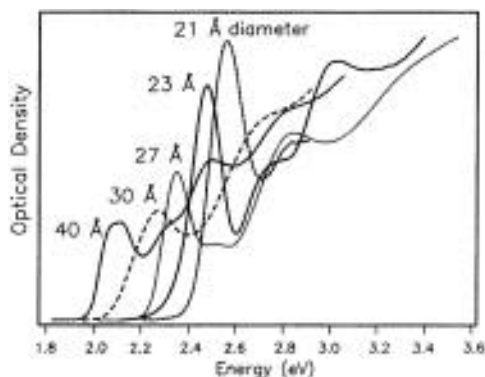


**Figure 16.** Optical absorption vs size for CdSe nanocrystals shows the shift to higher energy in smaller sizes, as well as the development of discrete structure in the spectra and the concentration of oscillator strength into just a few transitions.<sup>62</sup>

CdSe or InP.<sup>52</sup> As the size is reduced, the electronic states may be viewed as superpositions of bulk states. Hence, there is a shift to higher energy, the development of discrete features in the spectra, and concentration of the oscillator strength into just a few transitions. Qualitatively, all of these effects can be readily observed in the spectra of Figure 16, which show data for CdSe. The quantitative analysis of these spectra remains a difficult subject, for several reasons: The foregoing picture is a single-particle one and does not include the substantial effects of correlation. In molecules this is analogous to trying to use the highly approximate molecular orbital theory, instead of more advanced quantum chemistry methods. Regrettably, the nanocrystals are too large to describe using even moderately advanced methods that are routinely applied to small molecules. Further, in CdSe at least, the large atomic number of the Se ensures that the coupling between spin and orbital momenta is very strong in the valence bands (p bands).<sup>53–55</sup> This coupling is in the  $j-j$ , and not the Russell–Saunders,  $L-S$ , coupling regime. When translational symmetry is removed, the mixing of  $k$  vectors can also result in different bands mixing together. The shape of the crystallites, which is regular (tetrahedral, hexagonal prisms), or spherical, or ellipsoidal, will determine the symmetry of the nanocrystals and will influence the relative spacing of the levels. Finally, surface energy levels are completely excluded from this simple quantum confinement picture. Yet it seems apparent that surface states near the gap can mix with interior levels to a substantial degree, and these effects may also influence the spacing of the energy levels.<sup>56</sup> As of this writing, assignment of all the transitions remains a topic of research, but advances are occurring rapidly. Indeed, theoretical approaches that directly include the influence of the surface, as well as electronic correlation, are also being developed rapidly.<sup>57</sup>

#### Line Widths: Size Distributions and Intrinsic Broadening.

As a consequence of their being a new type of material, the properties of semiconductor nanocrystals can be expected to evolve with improvements in sample preparation. On the face of it, no property appears to have changed more in the past 10 years than the simple optical absorption spectrum. Spectra which at first seemed featureless and diffuse have gradually acquired definition, with multiple discrete states apparent in the latest generation of samples.<sup>55</sup> Essentially all of this progress derives from narrowing the distribution of sizes in the sample. Since the energies of the transitions depend so strongly on the size, size variation is a special form of inhomogeneous broadening at work here, which over time has been largely reduced. Today it is really the intrinsic, or single particle, line widths that are a matter of greater concern.

Ignoring for a moment the effects of the size distribution, it is of great importance to understand just how much oscillator strength can be compressed into a narrow region of the spectrum by the method of quantum confinement. In typical semiconductor nanocrystals, the energy level spacing is on the order of 0.15–0.3 eV. If the integrated oscillator strength over 0.15 eV of the bulk spectrum could be compressed into lines with widths on the order of 0.1–0.5 meV, nanocrystals would fulfill an important and new limit in nonlinear optical materials.<sup>58</sup> Recall that the polarizability scales with volume, so that the sharp, intense (radiative rates on the order of picoseconds) transitions of the nanocrystals could be readily manipulated by off-resonant electric fields. A prototype optical switch with gain, for instance, would be one in which the transmission of a high-power laser beam near the absorption threshold of the nanocrystals is modulated by a weaker, off-resonant pulse, via the ac Stark effect.

Many techniques have been employed to measure the average homogeneous spectra of nanocrystals, despite the presence of inhomogeneous broadening. These include transient hole burning,<sup>59,60</sup> luminescence line narrowing,<sup>56</sup> and photoluminescence excitation.<sup>55,56</sup> A direct measure of the average homogeneous line width comes from three-pulse photon echo experiments.<sup>61,62</sup> In these experiments, two pulses interfere in the sample to create a spatial grating. The third pulse scatters off this grating. When the delay between the first and third pulse is changed, the signal oscillates at the vibrational period of any vibrations which happen to be strongly coupled to the electronic excitation. For example, in high-quality CdSe nanocrystals, a single mode at  $210\text{ cm}^{-1}$  is observed in both the photon echo and resonance Raman experiments. When the first and second pulse are coincident in time, the maximum amplitude grating is prepared for the third pulse to scatter from. If the second pulse is delayed by more than the electronic dephasing time with respect to the first, then the amplitude of the grating will be greatly diminished. Thus, the intensity of the scattered light from the third pulse as a function of the delay between the first two pulses provides a measure of the homogeneous line width. This is shown in Figure 17A,B. The homogeneous line widths are extremely broad, corresponding to dephasing times on the order of 100 fs, with faster decays observed in smaller crystallites.

It is interesting to note that the coupling to the ionic lattice remains very strong even in small CdS<sup>63</sup> and CdSe nanocrystals. Simple models predict that as the semiconductor is reduced in size, coupling to the polar vibrations should be reduced, because the optically generated electron and hole are spatially coincident.<sup>64</sup> This clearly does not occur and suggests that other effects, such as the presence of polar crystallographic faces, may act to separate the optically generated electron–hole pair, even at the instant of optical excitation.<sup>7</sup>

In these experiments it proved possible to separate out all the contributions to the average homogeneous line width (Figure 18). Three mechanisms were shown to be important. The least important contribution came from lifetime broadening or population decay, which shows up as a fast recovery of the bleach induced by a single pulse and which is insensitive to the temperature. This corresponds to decay from the initially prepared electronic state into some other, for instance, a lower lying state that is optically forbidden<sup>65</sup> or a surface trap.<sup>56</sup> A somewhat more important mechanism of line broadening is dephasing by low-frequency acoustic modes (density fluctuations) of the crystallites. The contribution of this mechanism was identified via the strong temperature dependence of the dephasing time. This dephasing mechanism is significant, in that it appears to be intrinsic and not due to sample quality. When the electronic excitations are localized in a small volume,

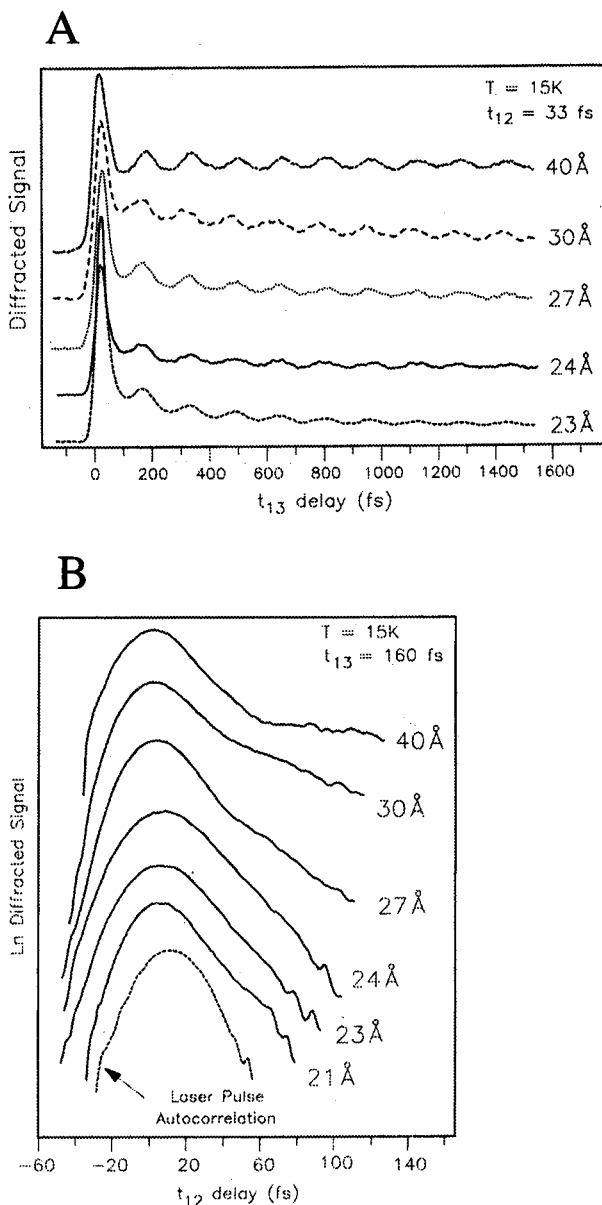


**Figure 17.** (A) Three-pulse photon echo experiments show the strength of the coupling of the electronic excitation to the relatively ionic nanocrystal lattice. In this experiment the delay between the first two pulses is fixed at 33 fs, and the diffraction intensity of the third pulse is measured as a function of the delay between the first and third. Strong coupling to a single mode at 210  $\text{cm}^{-1}$  shows up as a quantum beat.<sup>62</sup> (B) Measurement of the electronic dephasing time in CdSe nanocrystals by the three-pulse photon echo technique. In this case, the time between the first and third pulse is fixed, and the delay between the first two pulses is varied. The dephasing time is extremely fast, on the order of 100 fs for 22.6 Å diameter nanocrystals.

the coupling to the acoustic modes increases inevitably, placing a limit on the order of at least of a few microelectronvolts on the line widths of nanocrystals. Finally, there is a temperature-independent contribution to the dephasing time, which may be due to scattering off of surfaces or defects and which in principle at least may be eliminated by improvements in sample preparation.

As of this writing, the homogeneous line widths of nanocrystals remain a major topic of research. Vast improvements in the structural quality of samples, and in the size distributions, have resulted in no particular narrowing of the apparent homogeneous spectra. Furthermore, there appear to be some intrinsic limits to the narrowness of the lines in nanocrystals which arise from strong coupling to low-frequency vibrations. Currently, the spacings between nanocrystal electronic transi-

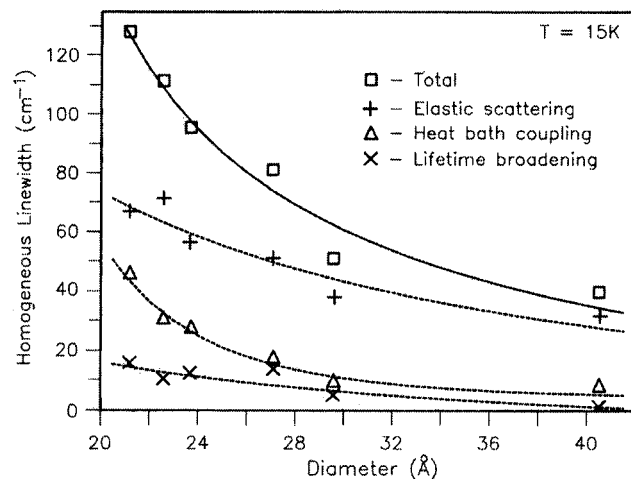


**Figure 18.** Different contributions to the total line width of CdSe nanocrystals, as determined in the three-pulse photon echo experiments.

tions appear to only slightly exceed the line widths, so that despite the large shifts to higher energy that are observed in the spectra, the idealized discrete spectra of Figure 2d appear not to be fully realized in practice. Further work, particularly in the area of inorganic passivation, is warranted.<sup>29</sup> Given the multiple sources of inhomogeneous broadening (size, shape, local fields, defects, etc.), the advent of single-molecule spectroscopy<sup>66,67</sup> and near-field scanning probe microscopy<sup>68</sup> shows great promise as tools to aid in deciphering the nature of the intrinsic photophysics of nanocrystals.<sup>69</sup>

#### Absorption and Emission in Indirect Gap Semiconductors.

One of the most interesting and current topics in the photophysics of semiconductor nanocrystals concerns the evolution with size of the indirect gap selection rule.<sup>70</sup> In Si and several other bulk semiconductors, the top of the valence band involves molecular orbitals that are in phase from unit cell to unit cell, while the bottom of the conduction band involves orbitals which switch sign from unit cell to unit cell (Figure 15B). The transition from the highest occupied level of the valence band to the lowest unoccupied level of the conduction band violates the  $\Delta k = 0$  selection rule imposed by translational symmetry and is therefore electronically forbidden and only weakly allowed vibronically. To see how this arises, consider the molecular orbitals pictured in Figure 15B, as well as the expression for the radiative rate in the bulk solid:

$$W = \int_f \left( \frac{2\pi}{\hbar} \right) \frac{|\langle \psi_{k \pm q, f} | H_{\text{el,phonon}} | \psi_{k, j} \rangle \langle \psi_{k, j} | e r | \psi_{k, i} \rangle|^2}{(E_{\text{gap}, k} - E_{\text{photon}})^2} \times \delta(E_f - E_i) \rho(E_f) dE_f$$

Since the net transition across the gap violates the bulk  $\Delta k = 0$  selection rule, imposed by translational symmetry, the transition is electronically forbidden. The transition may occur with phonon assistance, but the rate is lower than that of a direct gap transition by the square of the phonon scattering matrix element divided by  $(E_{\text{gap}} - E_{\text{photon}})^2$ , typically a factor of 1000 or so. The indirect gap selection rule arises from translational symmetry, and this can be seen by visual inspection of the molecular orbitals involved. The optical transition is electronically allowed within one unit cell. However, since  $\Delta k$  does not equal zero, the transition dipole moment points in different directions in adjacent unit cells. As a consequence, the electric field of light, whose wavelength is very long compared to unit cell dimensions, cannot couple to this transition. In the language of molecular spectroscopy, if the electronic transition is ac-

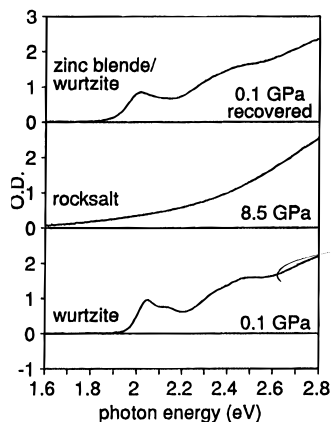


**Figure 19.** Electronic absorption spectra for CdSe nanocrystals in different crystallographic structures. In the four-coordinate wurtzite structure discrete features are evident. In the high-pressure rock salt structure the gap is much smaller, but no discrete features can be observed in the spectrum. This is due to a change in selection rule from direct to indirect when the local symmetry in the nanocrystal changes. When the pressure is released, the nanocrystals revert to a four-coordinate structure, and the discrete features are recovered.

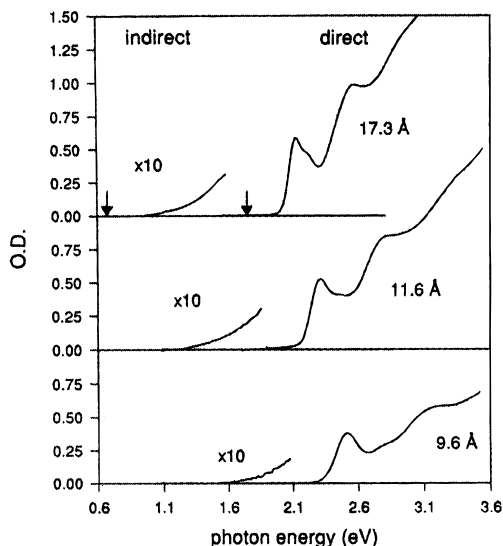


**Figure 20.** Electronic absorption spectra for three sizes of CdSe nanocrystals, in the wurtzite (direct) and rock salt (indirect) structures. In each instance the direct gap spectrum is structured and intense, while the indirect gap one is featureless and relatively weaker. The relative absorption efficiencies do not change, despite the concentration of oscillator strength due to quantum confinement.

accompanied by vibrational excitation of a mode with the proper symmetry, the transition may occur, and it is vibronically allowed, albeit much more weakly so than if it had been electronically allowed. The low radiative rate is observed for threshold excitation in absorption. At sufficiently high photon energies above the gap the density of states is large enough, or else vertical transition channels open up, so that the relative absorption efficiencies of direct and indirect gaps become comparable. As in molecules, however, higher electronic excitations in bulk semiconductors and nanocrystals rapidly relax to the gap. Thus, the low radiative rate in the indirect gap case is clearly manifested in emission, where the low radiative rates ensure that nonradiative processes dominate, and the quantum yields are low.<sup>71</sup>

Finite size disrupts translational symmetry but does not change the local bonding geometry. To a first approximation, the largest effect of quantum confinement is to change the density of states in the expression for the rate of photon absorption (and emission). When the position uncertainty is

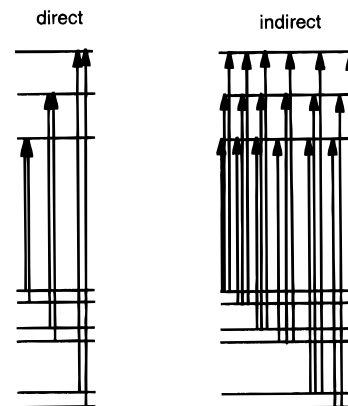


**Figure 21.** Qualitative comparison of the transitions in direct and indirect nanocrystals. In both instances the onset of absorption is shifted to higher energy due to quantum confinement. In the direct case, only a small number of transitions are strongly allowed (for instance transitions between states with the same envelope functions), leading to a nearly discrete spectrum. In the indirect case, all the transitions are electronically forbidden but weakly allowed vibronically. The absorptions are spaced more closely than the intrinsic transition line widths, so that the spectrum is effectively continuous.

reduced to  $\Delta x$ , energy levels of the nanocrystal may be described as superpositions of bulk energy levels within  $\Delta k$ , resulting in enhancements of the density of states at some energies and corresponding reductions elsewhere. The matrix elements which apply within the unit cell are basically unchanged. This can be seen clearly in a recent experiment, in which the absorption of CdSe nanocrystals in the direct-gap wurtzite structure is compared with the absorption of identically sized CdSe nanocrystals in the rock salt phase.<sup>72</sup> As was shown earlier, the nanocrystals can be converted from one structure to the other, without generation of defects, by application of external pressure. Since the average size, the size distribution, and the number of nanocrystals in the sample all remain constant during the transformation, these spectra provide a meaningful comparison of the effect of size on the selection rules (Figures 19 and 20). The degree of  $\Delta k$  mixing is identical, and in both structures this results in a shift of the threshold absorption to higher energy and an enhancement of the absolute threshold (band gap) radiative rate. Significantly, the *ratio* of the radiative rates remains unchanged. The “indirect gap” rock salt absorption is always a factor of 100 or more weaker than the “direct gap” wurtzite absorption. This demonstrates that the changes in the spectra arise from changes in the density of states, not changes in the matrix elements for absorption.

A further important difference between direct and indirect gap absorption spectra is preserved. In the direct gap case, the transitions are fundamentally electronic in nature, with weak vibrational sidebands. The electronic dipole selection rule ensures that only a small number of transitions between initial and final states are allowed, and the spectrum is relatively sparse. In the indirect gap case, every pairing of initial and final states can be rendered weakly allowed by the accompaniment of some appropriate vibration (Figure 21). Thus, the spectrum becomes highly congested with the spacing between the transitions significantly less than the intrinsic line widths. This is seen in Figure 20, where the wurtzite direct gap spectra are structured, while the rock salt indirect gap spectra are completely featureless. Interestingly, the discrete structure is even recovered when the pressure is lowered and a four-coordinate direct gap structure recovered. This proves that the absence of structure in the rock salt indirect gap phase is intrinsic.

Will there be a size below which the changes in the absorption and emission spectra of nanocrystals will be due to more than just changes in the density of states? In indirect gap materials,

the answer is surely yes. When the size of the crystallite is so small that it is only a few unit cells large, any selection rule that derives from translational symmetry will be strongly broken. In rock salt CdSe or in Si, the intrinsic matrix element for absorption, which is normally allowed in one unit cell, but rendered forbidden by translational symmetry, will again become electronically dipole allowed. There should be some size below which the featureless spectra characteristic of indirect gap materials break up into a series of discrete, allowed transitions. This has not been observed in any small indirect gap semiconductor to date. Even in Cd<sub>32</sub>S<sub>55</sub>,<sup>22</sup> which was recently investigated at high pressure in our laboratory in both structures,<sup>73</sup> this was not seen. This indicates how aptly the name nanocrystal is chosen: some vestiges of crystallinity or translational symmetry remain down to very small sizes.

The optical properties of indirect gap semiconductors, most notably of Si, have received enormous attention since the discovery of luminescence in porous Si.<sup>70,74</sup> In part, this reflected the hope that nanometer size Si crystallites would display allowed electronic transitions. In the event that this had been the case, the implication for optoelectronics would have been significant, since Si could then be used to transmit signals optically. In the end, it does appear as though the luminescence in Si nanocrystals derives partly from quantum confinement-induced enhancements in the radiative rate, but also from confinement-induced reductions in the nonradiative rate, which in bulk Si are dominantly due to three-body Auger effects.<sup>71</sup> In any event, the radiative rates for absorption and emission of light in Si, as in other indirect gap semiconductors, remain well below those of direct gap semiconductors, even in nanocrystals.

**Luminescence and Electroluminescence.** Narrow band (15–20 nm), size-tunable luminescence, with efficiencies at least of order 10%, is observed at room temperature from semiconductor nanocrystals. The origin of this luminescence remains the topic of some controversy. For some time researchers thought that this luminescence arose from partially surface trapped carriers.<sup>56</sup> Other experiments strongly suggest that the luminescence in fact arises from low-lying “dark” states of the nanocrystal interior, and surface modifications only influence the quantum yield by modulating the nonradiative rates.<sup>75</sup> Just as in organic molecules a singlet state may be optically prepared, followed by rapid relaxation to triplet states with long decay times, so in semiconductor nanocrystals, where  $j-j$  coupling dominates, an angular momentum allowed state is initially prepared, and on the time scale of picoseconds or longer, there is a decay to a lower lying angular-momentum-forbidden state, which decays relatively slowly (nanoseconds to microseconds). One success of this dark state model is the accurate prediction that the magnitude of the exchange splitting increases as  $r^{-3}$ , thus explaining one long puzzling feature of the luminescence. As the size is reduced, the shift between the absorbing and emitting state is observed to increase. The rigorous separation of interior and surface states is somewhat artificial in nanocrystals in any case, since substantial mixing may be expected. Indeed, other features of the spectra suggest that there may well be substantial surface character associated with the emitting state. For example, electric field modulation of the luminescence yields signals a factor of 100 or more larger than modulation of absorption, indicating that the emitting state is not as well confined spatially. Further evidence for surface localization of the emitting state comes from low-temperature studies of the vibronic coupling of the emission, which show that there is a well-defined localization temperature.

Independent of the exact origin of the luminescence, it does appear to be one property which can be manipulated in useful ways. For example, two reports of light-emitting diodes made

with polymers and CdSe nanocrystals have appeared within the past year.<sup>76,77</sup> In the first instance, nanocrystals were assembled in layers a few nanocrystals thick on the surface of PPV, an electroluminescent polymer. The PPV itself was grown on a layer of indium tin oxide, a transparent hole-injecting contact. Finally, the nanocrystal layer was coated with a film of Mg/Ag, the electron-injecting contact. This complete assembly electroluminesces when a voltage is applied. The recombination of electrons and holes may take place either in the polymer layer (which emits green light) or in the nanocrystal layer. The nanocrystal emission shifts with size. Thus, these LEDs provide a variety of means for tuning the output color. This advance is particularly important, since it constitutes the first example of *electrical*, rather than purely optical, investigation of semiconductor nanocrystals.

**Future Directions.** Advances in the science of semiconductor nanocrystals show no sign of abating. To the contrary, major goals which 10 years ago seemed unreachable today appear well within reach. In the next few years, one can expect steady improvements in the range of materials which can be prepared as nanocrystals, with the quality of group IV (Si, Ge) and III–V (InP, InAs, GaAs, GaP, ...) nanocrystals finally reaching the level of the prototypical II–VI materials. The properties of nanocrystals can be expected to improve dramatically, as faceted nanocrystals are routinely prepared, and the well-established methods of surface science are finally used to characterize reconstructions and chemisorption phenomena on individual crystallographic faces of nanocrystals. Passivation of nanocrystals with inorganic species, both disordered oxides, and epitaxially grown lattice matched layers will also continue to advance. At the same time, the current samples are of sufficient quality to enable a new generation of experiments. Nanocrystals will be integrated into electrical devices, a process which has only just begun. Current–voltage characteristics of nanocrystal monolayers and of individual nanocrystals will be measured. More complex assemblies of nanocrystals will be formed, including crystals of nanocrystals,<sup>78</sup> in which the spacing between crystallites may be altered at will, and nanocrystal molecules, in which nanocrystals of several different materials and sizes are linked together by organic molecules. New physics and chemistry are sure to be discovered as these complex assemblies of nanocrystals are investigated.

**Acknowledgment.** I would like to thank my students and co-workers. This work was supported by the Department of Energy, the National Science Foundation, and the Office of Naval Research Molecular Design Institute. The transmission electron micrographs were taken at the National Center for Electron Microscopy at the Berkeley National Lab. High-pressure diffraction data were taken using the UC/National Lab PRT beamline of the Stanford Synchrotron Radiation Lab.

## References and Notes

- (1) Vossmeier, T.; Katsikas, L.; Giersig, M.; Popovic, I. G.; Weller, H. *J. Phys. Chem.* **1994**, *98*, 7665.
- (2) Colvin, V. L.; Alivisatos, A. P.; Tobin, J. G. *Phys. Rev. Lett.* **1991**, *66*, 2786.
- (3) Goldstein, A. N.; Echer, C. M.; Alivisatos, A. P. *Science* **1992**, *256*, 1425.
- (4) Tolbert, S. H.; Alivisatos, A. P. *Annu. Rev. Phys. Chem.* **1995**, *46*, 595.
- (5) Murray, C. B.; Norris, D. B.; Bawendi, M. G. *J. Am. Chem. Soc.* **1993**, *115*, 8706.
- (6) Alivisatos, A. P. *Mater. Res. Soc. Bull.* **1995**, *20*, 23.
- (7) Shiang, J. J.; Kadavanich, A.; Grubbs, R. K.; Alivisatos, A. P. *J. Phys. Chem.*, in press.
- (8) Bawendi, M. G.; Kortan, A. R.; Steigerwald, M. L.; Brus, L. E. *J. Chem. Phys.* **1989**, *91*, 7282.
- (9) Wales, D. J.; Berry, R. S. *Phys. Rev. Lett.* **1994**, *73*, 2875. Berry, R. S. *Chem. Rev.* **1993**, *93*, 2379.

- (10) Ekimov, A. I.; Onushchenko, A. A. *Fiz. Tekh. Poluprovodn.* **1982**, *16*, 1215 (Translation: *Sov. Phys.—Semicond.* **1982**, *16*, 775).
- (11) Rossetti, R.; Nakahara, S.; Brus, L. E. *J. Chem. Phys.* **1983**, *79*, 1086.
- (12) Cohen, M. L.; Chou, M. Y.; Knight, W. D.; de Heer, W. A. *J. Phys. Chem.* **1987**, *91*, 3141. Wang, C. R. C.; Pollack, S.; Dahlseid, T. A.; Koretsky, G. M.; Kappes, M. *J. Chem. Phys.* **1992**, *96*, 7931. Ellert, C.; Schmidt, M.; Schmitt, C.; Reiners, T.; Haberland, H. *Phys. Rev. Lett.* **1995**, *75*, 1731.
- (13) Kastner, M. A. *Rev. Mod. Phys.* **1992**, *64*, 489.
- (14) Ralph, D. C.; Black, C. T.; Tinkham, M. *Phys. Rev. Lett.* **1995**, *74*, 3241.
- (15) Klein, D. L.; McEuen, P. L.; Bowen Katari, J. E.; Roth, R.; Alivisatos, A. P. A New Approach to Electrical Studies of Single Nanocrystals. *Appl. Phys. Lett.* **1996**, *68*, 2574.
- (16) This section, important for placing nanocrystals in a context, recently appears in abbreviated form: Alivisatos, A. P. *Science* **1996**, *271*, 993.
- (17) Liu, A.; Zhang, Q.-L.; Tittel, F. K.; Curl, R. F.; Smalley, R. E. *J. Chem. Phys.* **1986**, *85*, 7434.
- (18) Rothlisberger, U.; Andreoni, W.; Parrinello, M. *Phys. Rev. Lett.* **1994**, *72*, 665.
- (19) Arnold, C. C.; Neumark, D. M. *J. Chem. Phys.* **1993**, *99*, 3353.
- (20) The remarkable case of C<sub>60</sub>, discovered in molecular beam studies, but structurally characterized only after it could be produced in large quantities, demonstrates clearly the complementary roles played by gas and condensed phase studies of clusters.
- (21) Krautscheid, H.; Fenske, D.; Baum, G.; Semmelmann, M. *Angew. Chem., Int. Ed. Engl.* **1993**, *32*, 1303.
- (22) Herron, N.; Calbrese, J. C.; Farneth, W. E.; Wang, Y. *Science* **1993**, *259*, 1426.
- (23) Vossmeier, T.; Reck, G.; Katsikas, L.; Haupt, E. T. K.; *et al.* *Science* **1995**, *267*, 1476.
- (24) Steigerwald, M. L. *Polyhedron* **1994**, *13*, 1245.
- (25) Roth, J. D.; Lewis, G. J.; Safford, L. K.; Jiang, X. D.; Dahl, L. F. *J. Am. Chem. Soc.* **1992**, *114*, 6159.
- (26) Bowen Katari, J. E.; Colvin, V. L.; Alivisatos, A. P. *J. Phys. Chem.* **1994**, *98*, 4109.
- (27) Schuppler, S.; Friedman, S. L.; Marcus, M. A.; Adler, D. L.; Brus, L. E. *Phys. Rev. Lett.* **1994**, *72*, 2648. Wilson, W. L.; Szajowski, P. F.; Brus, L. E. *Science* **1993**, *262*, 1242. Littau, K. A.; Szajowski, P. J.; Muller, A. J.; Kortan, A. R.; Brus, L. E. *J. Phys. Chem.* **1993**, *97*, 1224.
- (28) Guzelian, A.; Bowen Katari, J. E.; Banin, U.; Alivisatos, A. P.; Heath, J. R. *J. Phys. Chem.* **1996**, *100*, 7212.
- (29) Schooss, D.; Mews, A.; Eychmuller, A.; Weller, H. *Phys. Rev. B: Condens. Matter* **1994**, *49*, 17072. Eychmuller, A.; Mews, A.; Weller, H. *Chem. Phys. Lett.* **1993**, *208*, 59.
- (30) Coombes, C. J. *J. Phys.* **1972**, *2*, 441.
- (31) Buffat, P.; Borel, J.-P. *Phys. Rev. A* **1976**, *13*, 2287.
- (32) Castro, T.; Reifengerger, R.; Choi, E.; Andres, R. P. *Phys. Rev. B: Condens. Matter* **1990**, *42*, 8548.
- (33) Beck, R. D.; St. John, P.; Homer, M. L.; Whetten, R. L. *Science* **1991**, *253*, 879.
- (34) Martin, T. P.; Naher, U.; Schaber, H.; Zimmermann, U. *J. Chem. Phys.* **1994**, *100*, 2322.
- (35) Couchman, P. R.; Jesser, W. A. *Nature* **1977**, *269*, 481.
- (36) Ercolessi, F.; Andreoni, W.; Tosatti, E. *Phys. Rev. Lett.* **1991**, *66*, 911.
- (37) Haase, M.; Alivisatos, A. P. *J. Phys. Chem.* **1992**, *96*, 6756.
- (38) Tolbert, S. H.; Alivisatos, A. P. *Science* **1994**, *265*, 373.
- (39) Herhold, A. B.; Alivisatos, A. P. *NATO Symp. Proc.*, in press.
- (40) Tolbert, S. H.; Herhold, A. B.; Brus, L. E.; Alivisatos, A. P. *Phys. Rev. Lett.*, submitted.
- (41) A general discussion of Peierls distortions in inorganic solids is presented in: Burdett, J. K. *Chemical Bonding in Solids*; Oxford University Press: New York, 1995.
- (42) Brus, L. E.; Harhless, J. A. W.; Stillinger, F. H. Theoretical Metastability of Semiconductor Crystallites in High Pressure Phases, with Application to beta-Tin Structure Silicon. *J. Am. Chem. Soc.*, in press.
- (43) Sachleben, J. R.; Wooten, E. W.; Emsley, L.; Pines, A.; Volvin, V. L.; Alivisatos, A. P. *Chem. Phys. Lett.* **1992**, *198*, 431.
- (44) Becerra, L.; Murray, C. B.; Griffin, R. G.; Bawendi, M. G. *J. Phys. Chem.* **1994**, *100*, 3297.
- (45) Majetich, S. A.; Carter, A. C.; Belot, J.; McCullough, R. D. *J. Phys. Chem.* **1994**, *98*, 13705.
- (46) Bowers, C. R.; Pietrass, T.; Barash, E.; Pines, A. *J. Phys. Chem.* **1994**, *98*, 9400.
- (47) Pietrass, T.; Pines, A.; Koch, V. P.; Alivisatos, A. P. *J. Non-Cryst. Solids*, in press.
- (48) Henglein A. Small-Particle Research—Physicochemical Properties of Extremely Small Colloidal Metal and Semiconductor Particles. *Chem. Rev.* **1989**, *89*, 1861.
- (49) Kortan, A. R.; Hull, R.; Opila, R. L.; Bawendi, M. G.; Steigerwald, M. L.; Carroll, P. J.; Brus, L. E. *J. Am. Chem. Soc.* **1990**, *112*, 1327. Hoener, C. F.; Allan, K. A.; Bard, A. J.; Campion, A.; Fox, M. A.; Mallouk, T. E.; Webber, S. E.; White, M. J. *J. Phys. Chem.* **1992**, *96*, 3812.
- (50) Hines, M. A.; Guyot-Sionnest, P. *J. Phys. Chem.* **1996**, *100*, 468.
- (51) Mews, A.; Kadavanich, A. V.; Banin, U.; Alivisatos, A. P. Structural and Spectroscopic Characterization of the CdS/HgS/CdS Quantum Dot Quantum Wells. *Phys. Rev. B*, in press.
- (52) Micic, O. I.; Sprague, J. R.; Curtis, C. J.; Jones, K. M.; *et al.* *J. Phys. Chem.* **1995**, *99*, 7754. Micic, O. I.; Curtis, C. J.; Jones, K. M.; Sprague, J. R.; *et al.* *J. Phys. Chem.* **1994**, *98*, 4966.
- (53) Efros, A. L. *Physica B* **1993**, *185*, 575. Efros, A. L.; Rodina, A. V. *Phys. Rev. B: Condens. Matter* **1993**, *47*, 10005.
- (54) Ekimov, A. I.; Hache, F.; Schanneklein, M. C.; Ricard, D.; *et al.* *J. Opt. Soc. Am. B: Opt. Phys.* **1993**, *10*, 100–107.
- (55) Norris, D. J.; Sacra, A.; Murray, C. B.; Bawendi, M. G. *Phys. Rev. Lett.* **1994**, *72*, 2612.
- (56) Bawendi, M. G.; Carroll, P. J.; Wilson, W. L.; Brus, L. E. *J. Chem. Phys.* **1992**, *96*, 946. Nirmal, M.; Murray, C. B.; Bawendi, M. G. *Phys. Rev. B: Condens. Matter* **1994**, *50*, 2293.
- (57) Hill, N. A.; Whaley, K. B. *Phys. Rev. Lett.* **1995**, *75*, 1130. Hill, N. A.; Whaley, K. B. *J. Chem. Phys.* **1994**, *100*, 2831. Wang, L. W.; Zunger, A. *Phys. Rev. Lett.* **1994**, *73*, 1039. Martin, E.; Delerue, C.; Allan, G.; Lannoo, M. *Phys. Rev. B: Condens. Matter* **1994**, *50*, 18258.
- (58) Schmitt-Rink, S.; Miller, D. A. B.; Chemla, D. S. *Phys. Rev. B: Condens. Matter* **1987**, *35*, 8113.
- (59) Alivisatos, A. P.; Harris, A. L.; Levinos, N. J.; Steigerwald, M. L.; Harris, T. D.; Brys, L. E. *J. Chem. Phys.* **1988**, *89*, 4001.
- (60) Esch, V.; Fluegel, B.; Khitrova, G.; Gibbs, H. M.; *et al.* *Phys. Rev. B: Condens. Matter* **1990**, *42*, 7450. Kang, K.; Kepner, A. D.; Hu, Y. Z.; Koch, S. W.; *et al.* *Appl. Phys. Lett.* **1994**, *64*, 1487.
- (61) Schoenlein, R. W.; Mittleman, D. M.; Shiang, J. J.; Alivisatos, A. P.; *et al.* *Phys. Rev. Lett.* **1993**, *70*, 1014.
- (62) Mittleman, D. M.; Schoenlein, R. W.; Shiang, J. J.; Colvin, V. L.; *et al.* *Phys. Rev. B: Condens. Matter* **1994**, *49*, 14435.
- (63) Shiang, J. J.; Risbud, S. H.; Alivisatos, A. P. *J. Chem. Phys.* **1993**, *98*, 8432.
- (64) Nomura, S.; Kobayashi, T. *Solid State Commun.* **1992**, *82*, 335. Nomura, S.; Kobayashi, T. *Phys. Rev. B: Condens. Matter* **1992**, *45*, 1305.
- (65) Efros, A. L.; Prigodin, V. N. *Appl. Phys. Lett.* **1993**, *62*, 3013.
- (66) Moerner, W. E. *Science* **1994**, *265*, 46.
- (67) Plakhotnik, T.; Moerner, W. E.; Palm, V.; Wild, U. P. *Opt. Commun.* **1995**, *114*, 83.
- (68) Trautman, J. K.; Macklin, J. J.; Brus, L. E.; Betzig, E. *Nature* **1994**, *369*, 40.
- (69) Blanton, S. A.; Dehestani, A.; Lin, P. L.; Guyot-Sionnest, P. *Chem. Phys. Lett.* **1994**, *229*, 317.
- (70) Cullis, A. G.; Canham, L. T. *Nature* **1991**, *353*, 335. Nash, K. J.; Calcott, P. D. J.; Canham, L. T.; Needs, R. J. *Phys. Rev. B: Condens. Matter* **1995**, *51*, 17698.
- (71) Brus, L. E.; Szajowski, P. F.; Wilson, W. L.; Harris, T. D.; *et al.* *J. Am. Chem. Soc.* **1995**, *117*, 2915.
- (72) Tolbert, S. H.; Herhold, A. B.; Johnson, C. S.; Alivisatos, A. P. *Phys. Rev. Lett.* **1994**, *73*, 3266.
- (73) Johnson, C. S.; Mizumoto, N. Private communication.
- (74) Koch, F.; Petrova Koch, V.; Muschik, T. *J. Lumin.* **1993**, *57*, 271.
- (75) Nirmal, M.; Norris, D. J.; Kuno, M.; Bawendi, M. G.; *et al.* *Phys. Rev. Lett.* **1995**, *75*, 3728.
- (76) Colvin, V. L.; Schlamp, M. C.; Alivisatos, A. P. *Nature* **1994**, *370*, 354–357.
- (77) Dabbousi, B. O.; Bawendi, M. G.; Onitsuka, O.; Rubner, M. F. *Appl. Phys. Lett.* **1995**, *66*, 1316.
- (78) Murray, C. B.; Kagan, C. R.; Bawendi, M. G. *Science* **1995**, *270*, 1335.